ELSEVIER

Journal of Chromatography A, 814 (1998) 43–54

JOURNAL OF CHROMATOGRAPHY A

Quasi-linear pH gradients for chromatofocusing using simple buffer mixtures: local equilibrium theory and experimental verification

Ronald C. Bates, Douglas D. Frey*

Department of Chemical and Biochemical Engineering, University of Maryland Baltimore County, Baltimore, MD 21250, USA

Received 27 February 1998; received in revised form 12 May 1998; accepted 12 May 1998

Abstract

Chromatofocusing utilizes internally generated, retained pH gradients to focus proteins into narrow chromatographic bands. One of the characteristics of current chromatofocusing methods is that they use expensive polyampholyte buffers containing large numbers of ill-defined components in order to generate linear or quasi-linear pH gradients. In addition to being costly to use, polyampholyte buffers also tend to associate with proteins and often yield irreproducible gradient shapes. In order to avoid the various difficulties associated with the use of polyampholyte buffers, this study investigates the use of mixtures of simple buffering species to generate quasi-linear pH gradients on a weak-base ion-exchange column packing. The ability of these gradients to separate protein mixtures was also investigated. To optimize the conditions used, a computer simulation method using a local equilibrium model was developed that predicts the shape of the pH gradient. Several experiments were performed that demonstrate the usefulness of the method and the accuracy of the model.

Keywords: Chromatofocusing; Gradient elution; pH gradients; Mobile phase composition; Proteins

1. Introduction

Ion-exchange chromatography is commonly used to separate proteins due to its simplicity, non-denaturing operating conditions and relatively low cost. In addition, ion-exchange chromatography is a well established unit operation for which a large body of mathematical modeling methods exists. In the late 1970s, Sluyterman and coworkers [1–3] described a method for producing internally generated, retained pH gradients in ion-exchange chromatography in order to separate proteins — a technique which they termed 'chromatofocusing'. The method involves presaturating an ion-exchange column at an initial pH, and then making a stepwise change to an elution buffer at a different pH. This causes a gradual pH gradient to form inside the column by virtue of the adsorption phenomena involved.

Chromatofocusing combines the high resolution of isoelectric focusing with the flexibility of ion-exchange chromatography to yield a purification method that is both efficient and easy to use. Chromatofocusing is most commonly used as an analytical method, although preparative scale versions of the technique have also been investigated [4–6]. Typically, analytical chromatofocusing has relied on the use of proprietary polyampholyte buffers and a weak-base ion-exchange adsorbent to create gradual pH profiles. However, polyampholyte buffers present numerous problems in use. Most importantly, they

*Corresponding author.

0021-9673/98/$19.00
PII: S0021-9673(98)00420-8

are a major expense if the method is used routinely. Furthermore, due to the way polyampholyte buffers are synthesized, lot-to-lot variations in properties exist, which lead to irreproducibilities when these materials are used in a chromatographic process. Finally, in some applications, polyampholyte buffering species are known to associate with proteins, leading to additional complications [7].

The objective of this investigation is to demonstrate a method that avoids these common problems by eliminating the use of polyampholyte buffers for producing quasi-linear pH gradients. Although previous workers have investigated the use of mixtures of chemically well-defined buffering species as a replacement for polyampholyte buffers, these previous studies have emphasized the use of large numbers of adsorbed buffering species, in which case the resulting sequence of stepwise pH transitions can be used to approximate a continuous pH gradient [4,7–10]. In contrast, in this study a gradual, nearly linear pH gradient will be produced by using a small number of non-adsorbed buffering species (i.e., buffering species that do not form an ion of the proper charge type to participate in ion exchange) and one inert adsorbed ion in the presaturation and elution buffers, and by optimizing the composition of these buffers. To perform the method, the column will be presaturated at an initial pH, and then eluted by a stepwise change to the elution buffer at a different pH, so that, as in traditional versions of chromatofocusing, the adsorption processes taking place inside the column are exploited to form a gradual pH gradient. The gradients produced in this way are shown here to be very reproducible. Furthermore, since the buffering species used are chemically well-defined, the performance of the method can be reliably predicted and optimized using a simple mathematical model.

A related version of the method proposed here which employs a sample-induced pH gradient has been described by Slais [11]. However, the method developed in this study is simpler to implement and produces quasi-linear pH gradients in a more flexible and controllable manner. Related work, which has evidently never been published, has also been described by Kirsch [12]. It should also be noted that a number of studies have investigated the use of linear pH gradients produced by the mixing of buffers external to the column (see, e.g., [13]). In comparison to those studies, the methods developed in this work are simpler to implement since they employ stepwise changes from the elution to the presaturation buffers. Furthermore, internally produced pH gradients of the type used in this study tend to be less denaturing than externally produced gradients since, in general, they minimize the amount of time that proteins are exposed to pH extremes.

2. Experimental

2.1. Materials and methods

Weak-base ion-exchange adsorbents (PBE 94 and PBE 118, Pharmacia) were packed into Omnifit borosilicate glass columns (250×6.6, 100×6.6 and 250×10 mm) purchased from Rainin. Prefiltering and degassing of the buffers were accomplished by vacuum filtration using a 0.2-μm pore size, 47 mm diameter filter composed of nylon 66 and obtained from Rainin. The chromatography equipment was obtained from Thermo Separation Products, and includes a vacuum degasser, a SpectraSystem P4000 pump and a SpectraSystem UV2000 UV/Vis detector. The pH of the eluent was measured using an on-line sampling cell and either an Orion Model 91-03 pH minielectrode or a Sensorex Model 450 CD pH electrode attached to an Orion Model 701A Ionalyzer. Both the pH meter and the UV detector were connected via STRAWBERRY TREE DATASHUTTLE and STRAWBERRY TREE WORKBENCH software to an IBM personal computer for real time data acquisition. All chemicals and proteins were purchased from Sigma. Buffers were made by adding a known weight of each buffering species to a known volume of prefiltered, deionized water. The solution was then titrated with HCl to the appropriate pH. Prior to use, all buffers were vacuum filtered again, as described above.

3. Theory

3.1. Material balance relations for an adsorbed ion

It will be assumed in this study that mass transfer is sufficiently fast so that equilibrium exists at each

point throughout the column, and that the effects of axial dispersion are negligible. Consider an adsorbed ion, such as the chloride ion, that is chemically inert in the sense that it does not form other chemical species by the addition or removal of the hydrogen ion. The velocity that a concentration level of this adsorbed inert ion travels through the column, termed here the concentration velocity v_C, is given by the following relation, which results from material balance considerations [14]:

$$v_C = \frac{v_{\text{fluid}}}{1 + \dfrac{(1-\alpha)}{\alpha}\dfrac{dq^*_{S^-,t}}{dC_{S^-}}} \quad (1)$$

In Eq. (1), the subscript t denotes that a quantity is based on total amounts within the exterior surface of the particle, the superscript * denotes an equilibrium value, and the subscript S^- denotes the inert ion. In contrast, unadsorbed buffering species and inert ions travel through the column at the fluid velocity and, therefore, have the same liquid phase concentration as in the elution buffer for regions where $t > z/v_{\text{fluid}}$, where z is the distance from the column inlet and t is the time from the start of the elution step. Conversely, for regions where $t < z/v_{\text{fluid}}$, the presaturation conditions prevail for the unadsorbed species. If the column is uniformly presaturated, and if there is a stepwise change to an elution buffer at $t=0$, then the time for a concentration level to elute from the column is given by L/v_c, where L is the column length, and the dimensionless elution time is given by v_{fluid}/v_c, or equivalently, by tv_{fluid}/L. Note that the presence of unadsorbed buffering species and inert ions in the particle pores is ignored in this development.

3.2. Golden's rule

Adsorption isotherms can be categorized into three major classes; i.e., those with no inflection point, those with one inflection point, and those with multiple inflection points. In the simplest case of no inflection points, the isotherm is either concave upward, indicating the isotherm is unfavorable for adsorbate uptake, concave downward, indicating the isotherm is favorable for adsorbate uptake, or the isotherm is linear. Eq. (1) can be applied in a straightforward manner to an isotherm that is unfavorable for solute uptake and where the solute has a higher concentration in the elution buffer than in the presaturation buffer by evaluating the isotherm slope at each concentration level. However, for a favorable isotherm under the same presaturation and elution conditions, Eq. (1) predicts that downstream concentration velocities are faster than upstream concentration velocities, which is physically impossible. The physically correct profile corresponds instead to a cord connecting the feed and presaturation points, i.e., to a step change in concentration. The cord therefore becomes an effective isotherm to which Eq. (1) can be applied by replacing the derivatives in that equation with $\Delta q_{S^-,t}/\Delta C_{S^-}$, where $\Delta q_{S^-,t}$ and ΔC_{S^-} are the changes in the adsorbed and liquid-phase concentrations for the inert ion across the step change.

In many cases of practical interest, the isotherm of an adsorbed ion exhibits an inflection point. Such isotherms, known as composite isotherms, may exhibit both favorable and unfavorable regions. In systems characterized by a composite isotherm, the effective isotherm for calculating concentration velocities is determined by the so-called Golden's rule [15,16], which states that the effective isotherm can be constructed by fixing one end of a hypothetical string at the elution conditions (point E in Fig. 1a) and then stretching the string around the isotherm in a clockwise direction from the elution conditions to the presaturation conditions (point P), as illustrated in Fig. 1a. The region where the string hugs the isotherm represents a gradual transition so that the instantaneous slope of the isotherm determines the concentration velocity at each point. The region where the string does not hug the isotherm, i.e., the region from point A to point P in Fig. 1, corresponds to a step change in concentration, and the slope of the corresponding chord (i.e., $\Delta q_{S^-,t}/\Delta C_{S^-}$) determines the velocity of that step change.

Fig. 1 shows an example of the application of Golden's rule as just described to an isotherm containing one inflection point. The isotherm shown corresponds to the adsorption of the chloride ion on the PBE 118 column packing in the presence of a fixed liquid phase concentration of three cation-forming buffering species. A more detailed discussion of the adsorption behavior corresponding to this example is given in Section 4.2. For isotherms containing multiple inflection points, the same gener-

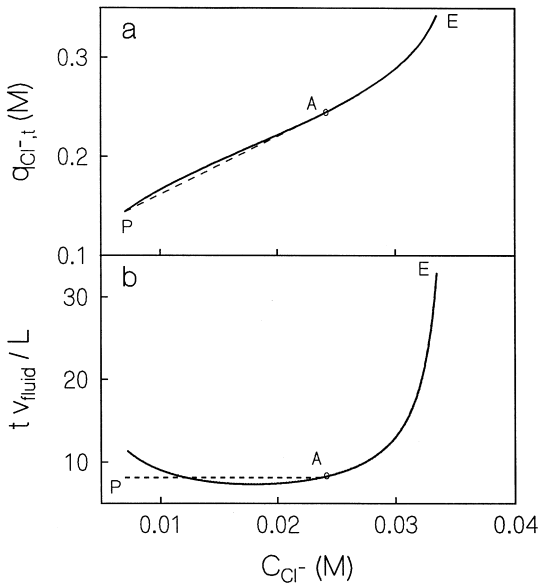

Fig. 1. Illustration of Golden's rule applied to the adsorption isotherm for the chloride ion on PBE 118 in the presence of a fixed concentration of three unadsorbed buffering species. Point P corresponds to the presaturation condition, point E corresponds to the elution condition and point A is the point where a hypothetical stretched string would leave the isotherm. The solid line in Fig. 1a is the actual adsorption isotherm, and the dotted line is the effective isotherm determined using Golden's rule. The solid line in Fig. 1b is the effluent concentration profile that would result if the actual adsorption isotherm in Fig. 1a was used to calculate the concentration velocity, whereas the dotted line in Fig. 1b corresponds to the profile that results from using the effective isotherm in Fig. 1a. Physical properties used in the calculations are described in the caption to Fig. 5.

al approach can be used to determine the effective isotherm and, hence, the effluent concentration profile for the adsorbed inert ion which, under these conditions, may contain multiple gradual and abrupt sections.

Golden's rule yields an effective isotherm from an actual isotherm; however, before this rule can be applied, the actual isotherm needs to be determined for the conditions that apply. This can be done in the present case by titrating the column packing batchwise with the adsorbed inert ion in the form of a strong acid, and then fitting the titration data to a physical model for the adsorption isotherm. The model can then be used to calculate theoretically the adsorbed phase compositions at equilibrium for a specified liquid phase composition, as discussed in the following sections.

3.3. Liquid phase acid–base equilibrium

This study considers the case of an anion-exchange column and a liquid phase that contains several unadsorbed (i.e. cation-forming) buffering species and one adsorbed inert anion. Acid–base equilibrium for a buffering species which involves equilibrium between a cationic and a neutral form, is governed by the following chemical equation:

$$A_i^+ \rightleftharpoons A_i^0 + H^+ \tag{2}$$

The acid–base equilibrium constant for Eq. (2) is defined as:

$$K_{A_i} = C_{A_i^0} C_{H^+} / C_{A_i^+} \tag{3}$$

The following relations result from rearranging Eq. (3) and using a species balance to introduce the total amount of the buffering species C_{A_i}:

$$C_{A_i^+} = \frac{C_{H^+} C_{A_i}}{K_{A_i} + C_{H^+}} \tag{4}$$

$$C_{A_i^0} = \frac{K_{A_i} C_{A_i}}{K_{A_i} + C_{H^+}} \tag{5}$$

The electroneutrality condition can be written for the liquid phase as:

$$C_{H^+} - \frac{K_W}{C_{H^+}} - C_{S^-} + \sum_i C_{A_i^+} = 0 \tag{6}$$

Replacing the summation in Eq. (6) with the appropriate relations for the concentrations of the positively charged buffering species from Eq. (4), and assuming that the liquid phase concentration of the inert anion is known, yields an equation with the liquid phase hydrogen ion concentration as the only unknown. The liquid-phase hydrogen ion concentration determined from this equation can then be substituted into Eqs. (4) and (5) to determine the concentrations of the charged and neutral forms of the buffering species. This procedure yields the pH and the concentrations of all forms of the buffering species in the liquid phase given the total concentrations of the buffering species and the concentration of the inert anion in the liquid phase. The

method described here for calculating these quantities can easily be extended to include the presence of acidic buffering species, acidic or basic buffering species with more than two ionic forms, and the presence of inert cations.

3.4. Interphase adsorption equilibrium

Ion-exchange equilibrium expressions can be formulated by equating the chemical potentials of neutral combinations of ions in the adsorbed and fluid phases [4–6,17]. When the hydrogen ion is used to form these neutral combinations, the following relation results:

$$q_{H^+,t}^{-z_{S^-}} q_{S^-,t} = K_{S^-,t} C_{H^+}^{-z_{S^-}} C_{S^-} \quad (7)$$

Since in the present case $z_{S^-} = -1$, Eq. (7) yields:

$$q_{S^-,t} = K_{S^-,t} C_{S^-} C_{H^+} / q_{H^+,t} \quad (8)$$

Conversely, the adsorption of neutral forms of the buffering species can be ignored in this development due to the fact that these species affect neither the charge balance nor the amount of inert anion adsorbed.

If it is assumed that the weak-base functional groups attached to the column packing are noninteracting and follow simple acid–base equilibrium, then the total concentration of ionized functional groups on the adsorbent at any adsorbed phase hydrogen ion concentration is given by:

$$q_{R^+t} = \sum_j q_{R_j^+t} = \sum_j \frac{q_{H^+,t} + q_{R_j,t}}{K_{R_j} + q_{H^+,t}} \quad (9)$$

where $q_{R_i,t}$ and K_{R_j} are determined from batch titrations of the adsorbent as explained below. Furthermore, if the electroneutrality condition is written for the adsorbed phase, an equation having the adsorbed phase hydrogen ion concentration, $q_{H^+,t}$, as the only unknown results:

$$q_{H^+,t} i - \frac{K_w}{q_{H^+,t}} - \frac{K_{S^-,t} C_{S^-} C_{H^+}}{q_{H^+,t}} + \sum_j \frac{q_{H^+,t} + q_{R_j,t}}{K_{R_j} + q_{H^+,t}} = 0 \quad (10)$$

Provided that the liquid phase composition is specified so that all of the ionic species in the liquid phase can be determined as described above, then Eq. (10) can be solved for $q_{H^+,t}$, and this value can be substituted into Eq. (8) to determine the amount of inert ion present in the adsorbed phase.

4. Results

4.1. Batch titrations

Batch titrations of the PBE 94 and PBE 118 column packings were performed in order to determine the adsorption equilibrium properties of these materials. To perform the titration of PBE 94, the column packing was first equilibrated with 1 *M* KCl, adjusted to pH 3 with HCl by repeated batch contacting. Next, a measured quantity of the adsorbent was added to a flask containing a known quantity of 1 *M* KCl at pH 3. Small quantities of 0.442 *M* NaOH were then added to the flask and the pH was measured subsequently. Results are shown in Fig. 2 for PBE 94 and indicate that the functional groups attached to the PBE 94 column packing are titrated evenly over the complete operating range of the adsorbent.

To determine the values of q_R and $K_{Cl^-,t}$ for the PBE 94 column packing, it was assumed that the adsorption properties of this material could be represented by a spectrum of noninteracting functional groups all having the same concentration, and whose pK_a values are evenly distributed from 3 to 13. The best fitting values of q_R and $K_{Cl^-,t}$ were determined as the values which, for all the data sets, minimized the discrepancy between the values of q_{Cl^-} determined from a material balance using the data in Fig. 2, and the values determined from Eqs. (8) and (10). For PBE 94, these best fitting values corresponded to a total titratable capacity of 0.75 *M* in the pH range between 3 and 13, and a value of 0.85 for $K_{Cl^-,t}$.

The PBE 118 column packing was characterized in a similar manner, except that, in this case, the titration curve was not linear, as shown in Fig. 2. The curve could, however, be represented by three different linear regions, each of which was analyzed as discussed above.

4.2. pH gradient generation

The local equilibrium (LEQ) model described in

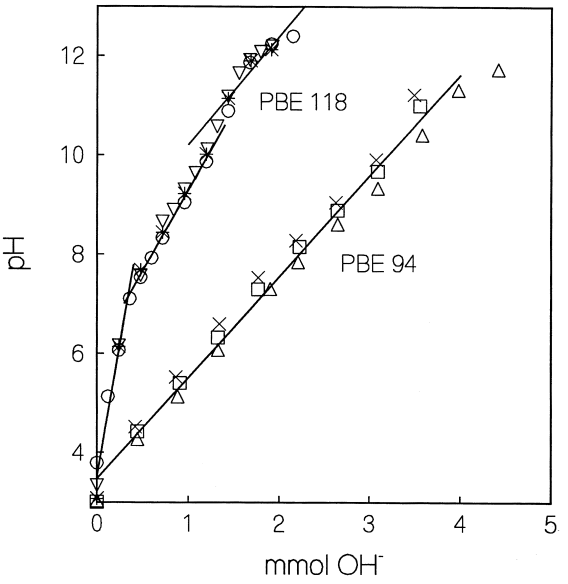

Fig. 2. Titration of PBE 94 and PBE 118 performed by taking a known quantity of the adsorbent, initially equilibrated with 1 *M* KCl at pH 3, and then titrating it batchwise with 0.442 *M* NaOH (for PBE 94) and 0.239 *M* NaOH (for PBE 118). The symbols represent data from three separate titrations, and the lines represent a linear regression fit of all three data sets. The data for PBE 118 were assumed to fall into three linear regions with the lines shown representing linear regression fits in those regions.

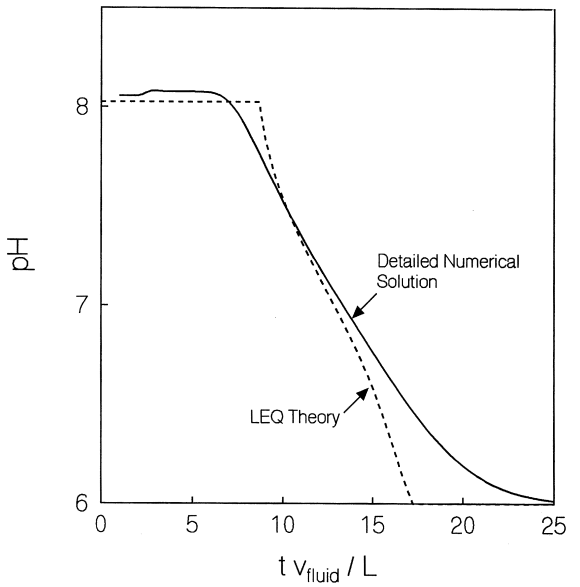

Fig. 3. Effluent pH profile for a hypothetical weak-base anion-exchange column packing having functional groups with pK_a values of 9.6, 8.6 and 7.6, and concentrations of 0.3333 *M* each. The presaturation and elution buffers contain weak-base buffering species with pK_a values of 8, 7 and 6 at concentrations of 0.1, 0.0362 and 0.0362 *M*, respectively. The adsorption equilibrium constant for the inert anion was assumed to be unity, and the interstitial porosity (or void volume) was assumed to be 0.35 in the calculations. For the detailed numerical calculations, the intraparticle diffusion coefficient used for all of the buffering species and for the chloride ion was 10^{-6} cm^2/s, and the adsorption equilibrium constants for the neutral and positive forms of the buffering species were assumed to be unity.

Section 3 was used to investigate the effect of the buffer composition on the shape of the pH gradient for the case where a weak-base anion-exchange column was employed together with weak-base (i.e., cation-forming) buffering species and one adsorbed inert anion (i.e., the chloride ion). The main result of these investigations is illustrated in Fig. 3, which indicates that when the physical properties and concentrations of the buffering species for this system are properly chosen, a retained pH gradient can be formed which is continuous and nearly linear in shape. Fig. 3 in particular shows local equilibrium theory results for a hypothetical set of buffering species, together with results from a detailed numerical calculation for the same set of conditions, but with mass transfer resistances and the relatively minor amounts adsorbed of the neutral and positively charged forms of the buffering species included in the calculation. The numerical calculations were performed using the method of characteristics as described by Frey et al. [4] and Strong and Frey [6].

It can be noted from Fig. 3 that the main effect of incorporating mass transfer resistances into the calculation procedure is to broaden the pH profile to a minor degree, but without changing the basic shape of the profile, while the effect of incorporating the adsorption of neutral and positively charged forms of the buffering species is to shift by a minor amount the entire pH profile to longer times.

The sample calculations shown in Fig. 3 involve the case where the presaturation and elution buffers contain identical concentrations of basic buffering species titrated to different pH values using a strong acid. Under these conditions, a single pH transition forms which separates the presaturation and elution pH plateaus. In the more general case, however, the presaturation and elution buffers, although containing a common inert anion that adsorbs onto the

column packing, may differ with regard to the concentrations and identities of the unadsorbed basic buffering species present. In that case, two pH transitions are formed, separated by an intermediate pH plateau. The first of these pH transitions to exit the column is a transition in which the unadsorbed buffering species in the presaturation buffer are replaced by the buffering species present in the elution buffer. This transition necessarily travels at the velocity of an unadsorbed solute, i.e., it is the 'fast' or 'unretained' transition and, according to Eq. (1), it is characterized by the same value for the amount of adsorbed inert anion on the upstream and the downstream sides of the transition. The second transition to exit the column travels more slowly than an unadsorbed solute, i.e., it is the 'slow' or 'retained' transition, which is characterized by a fixed concentration for all of the unadsorbed buffering species.

In order to represent possible fast and slow transitions for a range of conditions, it is convenient to plot fast and slow 'paths' on an appropriate composition diagram, where the fast paths connect possible combinations of presaturation and intermediate plateaus and the slow paths connect possible combinations of intermediate and elution plateaus. The entire pH profile can then be determined by locating the presaturation plateau on the diagram and following the fast path to where it intersects the slow path emanating from the elution plateau. The intersection gives the conditions of the intermediate plateau while the fast and slow paths themselves describe conditions along the fast and slow transitions due to the fact that any composition on either of these two transitions is potentially an intermediate plateau corresponding to some particular elution and presaturation conditions.

Fig. 4 illustrates a composition diagram of the type just described, where the vertical axis is the liquid phase pH and the horizontal axis is the liquid phase concentration of the inert anion present. The slow paths on the figure correspond to elution buffers that contain fixed ratios of three different buffering species, but varying total concentrations for those species, while the fast paths are characterized by fixed values for q_{Cl^-} and account for the fact that the column can be presaturated with a buffer containing an arbitrary mixture of unadsorbed buffering species,

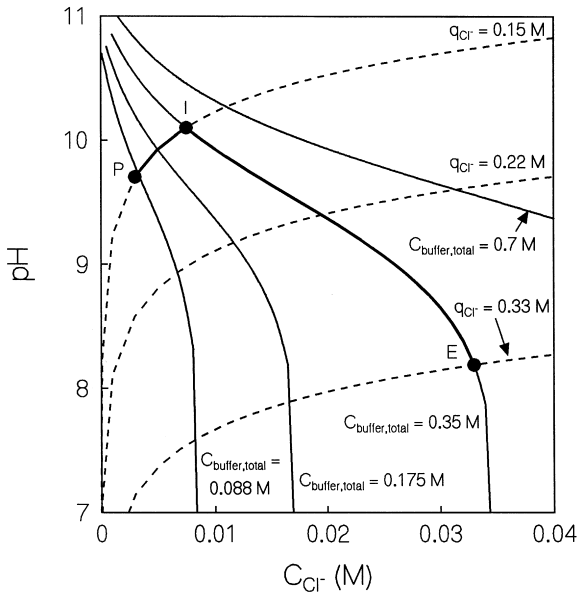

Fig. 4. Fast and slow composition paths (dashed and solid lines) for a system with the chloride ion as the only adsorbed ion and with three cationic buffering species. The fast paths represent constant adsorbed phase chloride ion concentrations in the PBE 118 column packing, and the slow paths correspond to the case where ethanolamine, trimethylamine and diethanolamine are present in the ratio 4:2:1 and with the total concentration indicated. Points P, I and E represent the presaturation conditions, intermediate plateau and the elution conditions, respectively, that were used in Figs. 1 and 5. Physical properties used in the calculations are described in the caption to Fig. 5. Note that the point 'P' in Fig. 1 corresponds to the point 'I' in Fig. 4.

provided that the proper presaturation pH is attained by titrating that buffer with the inert anion in the form of a strong acid. The conditions used to construct the various paths in Fig. 4 correspond to those used in Fig. 1, and the specific elution and presaturation conditions illustrated by the points E and P in Fig. 4 yield the retained front specifically illustrated in Fig. 1.

Fig. 5 illustrates the experimentally measured and theoretically predicted effluent pH profiles corresponding to the conditions of Figs. 1 and 4. As shown, a quasi-linear pH gradient was produced on the PBE 118 column packing. The figure also indicates that the experimentally measured pH profile compares well with those predicted theoretically using the adsorption equilibrium data for the chloride ion illustrated in Fig. 2. To produce the pH gradient

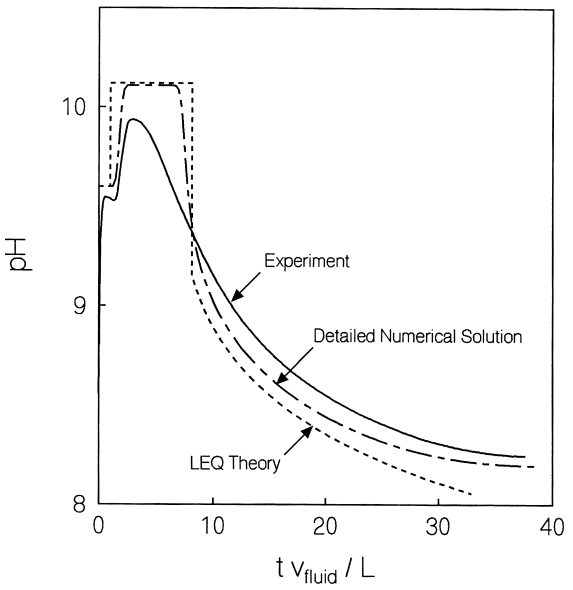

Fig. 5. Effluent pH profile obtained using a 16×0.66 cm column packed with PBE 118. The adsorbent was presaturated with 0.005 *M* ethanolamine titrated to pH 9.6 with HCl and eluted at a flow-rate of 1.0 ml/min with a buffer containing 0.02 *M* ethanolamine, 0.01 *M* trimethylamine and 0.005 *M* DEA. The pK_a values used for the buffering species in the calculations were 9.5, 9.8 and 9.1, respectively. The adsorption equilibrium constant for the chloride ion was assumed to be 0.85, and the total capacity of the adsorbent was taken as 0.659 *M*. The total capacity was subdivided as suggested by the three linear regions of Fig. 2, and the functional groups attached to the adsorbent were assumed to have equal capacities within each region. Region 1, with functional groups having pK_a values from 3.5 to 7, was assumed to have a total capacity of 0.128 *M*, region 2, with pK_a values ranging from 7.5 to 10, was assumed to have a capacity of 0.3 *M* and region 3, with pK_a values ranging from 10.5 to 13, was assumed to have a capacity of 0.231 *M*. The LEQ results shown correspond to those illustrated in Figs. 1 and 4. For the detailed numerical calculations, the intraparticle diffusion coefficient used for all the buffering species and for the chloride ion was 10^{-6} cm^2/s, and the adsorption equilibrium constants for the neutral and positive forms of the buffering species were assumed to be unity.

shown, the column was first presaturated with a buffer containing ethanolamine, and then eluted with a buffer that contained a mixture of ethanolamine, trimethylamine and diethanolamine (DEA). Note that the shape of the pH profile is similar to the profile shown in Fig. 3, except that an initial rise in pH occurs before the downward pH gradient begins. The rise in the pH results from the presence of an unretained front in which the mixture of ethanolamine, trimethylamine and DEA replaces the original ethanolamine in the presaturation buffer, as discussed above.

Fig. 6 illustrates calculation results for the case where a PBE 94 column is eluted with a mixture of bis[2-hydroxyethyl]imino–tris[hydroxymethyl]-methane (Bis–Tris), piperazine and *n*-methyl-piperazine at a fixed ratio, but with varying total concentrations, as indicated. The particular presaturation and elution conditions shown in the figure are for the simplified case where the presaturation condition (point P) and the elution condition (point E) lie on the same slow path, so that there is no initial change in pH before the retained pH transition elutes from the column. The adsorption isotherm for the presaturation and elution conditions shown in Fig. 6 contains no inflection point and exhibits a concave upward shape, as seen in Fig. 7. Fig. 7b shows the result of applying Golden's rule to the adsorption

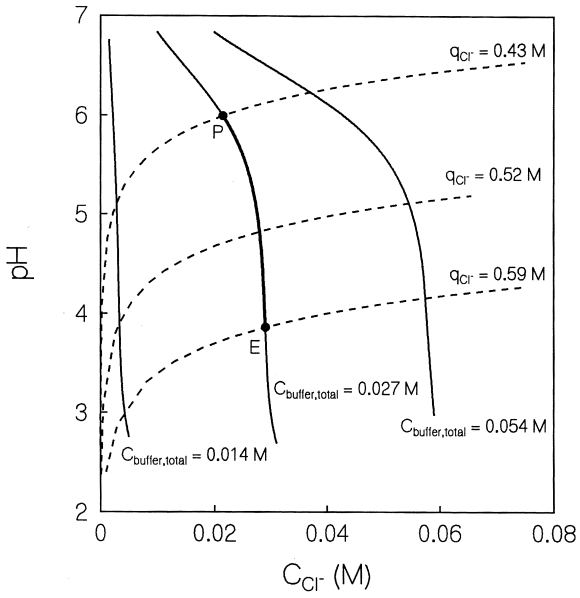

Fig. 6. Fast and slow composition paths (dashed and solid lines) for a system with the chloride ion as the only adsorbed ion and with three cationic buffering species. The fast paths represent constant adsorbed phase chloride ion concentrations on the PBE 94 column packing and the slow paths correspond to the case where Bis–Tris, piperazine and *n*-methyl-piperazine are present in the ratio 25:1:1 and with the total concentration shown. Points P and E represent the presaturation and elution conditions, respectively, used in Figs. 7 and 8. Physical properties used in the calculations are described in the caption to Fig. 8.

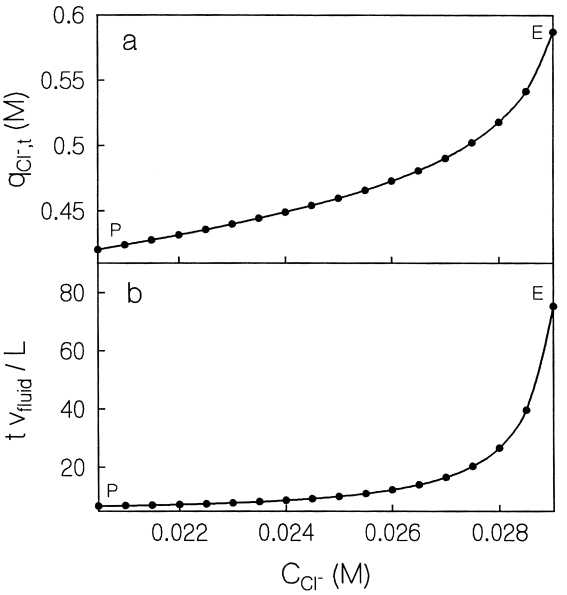

Fig. 7. Illustration of Golden's rule applied to an adsorption isotherm containing no inflection points, which is unfavorable for solute uptake. The conditions correspond to those used in Figs. 6 and 8. The solid line in Fig. 7a is the actual adsorption isotherm, while the solid circles correspond to the effective isotherm determined using Golden's rule. The solid line in Fig. 7b denotes the effluent concentration profile that results if the actual isotherm in Fig. 7a is used to calculate the concentration velocity, while the solid circles in Fig. 7b denote the profile that results from using the effective isotherm in Fig. 7a to calculate the concentration velocity. Physical properties used in the calculations are described in the caption to Fig. 8.

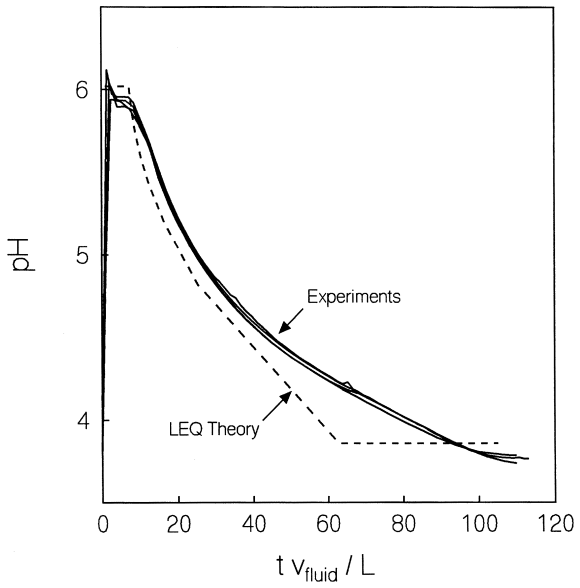

Fig. 8. Effluent pH profile obtained using a 5×0.66 cm column packed with PBE 94. The adsorbent was presaturated with 0.025 *M* Bis–Tris titrated to pH 6 with HCl and eluted at a flow-rate of 1.0 ml/min with a buffer containing 0.025 *M* Bis–Tris, 0.001 *M* piperazine and 0.001 *M* *n*-methylpiperazine. The pK_a values for the buffering species are 6.5, 5.8 and 4.75, respectively. Piperazine and *n*-methylpiperazine each have an additional (i.e., third) charged form with pK_a values of 9.8 and 9.2, respectively. The total capacity of the adsorbent and the chloride ion equilibrium constant for adsorption were 0.75 *M* and 0.85, as determined from the batch titration shown in Fig. 2.

isotherm shown in Fig. 7a, which was calculated from the data for the adsorption of the chloride ion on PBE 94 shown in Fig. 2. Unlike the isotherm shown in Fig. 1, the curve generated by Golden's rule never leaves the isotherm in Fig. 7, so that an entirely gradual pH change is predicted for the retained transition.

Fig. 8 illustrates a comparison of experimentally measured and theoretically predicted effluent pH profiles for the case shown in Figs. 6 and 7, where a column packed with PBE 94 was presaturated at pH 6.0 with a buffer containing Bis–Tris, and then eluted with an elution buffer at pH 3.8 containing Bis–Tris as well as two additional weak-base buffering species. As shown in the figure, under the conditions employed, a retained pH gradient is produced having a shape of the type often desired for separating proteins at the analytical scale, i.e., it is entirely gradual in shape and becomes progressively shallower as the elution time increases. Fig. 8 also shows the result of four duplicate experiments, a comparison of which indicates that retained, gradual pH gradients can be formed in a highly reproducible manner under the conditions used.

Fig. 9 illustrates a composition diagram for a relatively complicated case involving the use of the PBE 94 column packing together with two cation-forming buffering species, and with the chloride ion again as the adsorbed ion. The adsorption isotherm corresponding to the presaturation and elution conditions shown in Fig. 9 is illustrated in Fig. 10. Concentrations for the buffering species in the elution buffer where chosen so that a composite adsorption isotherm having three inflection points for the chloride ion is produced, and Golden's rule is

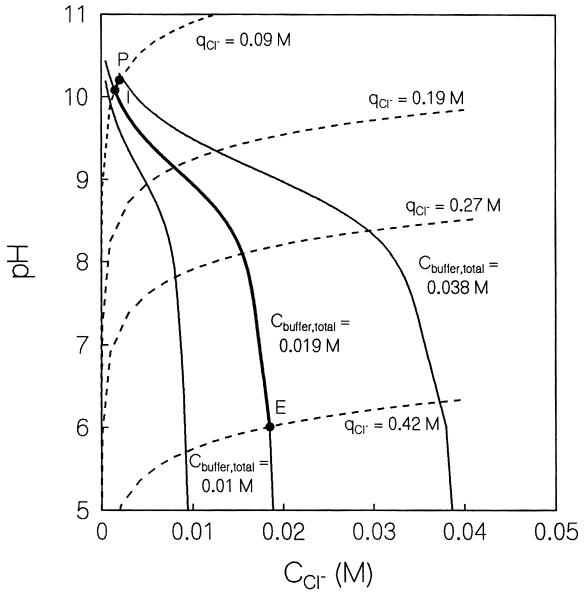

Fig. 9. Fast and slow composition paths (dashed and solid lines) for a system with the chloride ion as the only adsorbed ion and with two cationic buffering species. The fast paths represent constant adsorbed phase chloride concentrations and the slow paths correspond to the case where diethanolamine and Bis–Tris are present in the ratio 17:2 and with the total concentration shown. Points P, I and E represent the presaturation, intermediate plateau and the elution conditions, respectively, that were used in Figs. 10 and 11. Physical properties used in the calculations are described in the caption to Fig. 11.

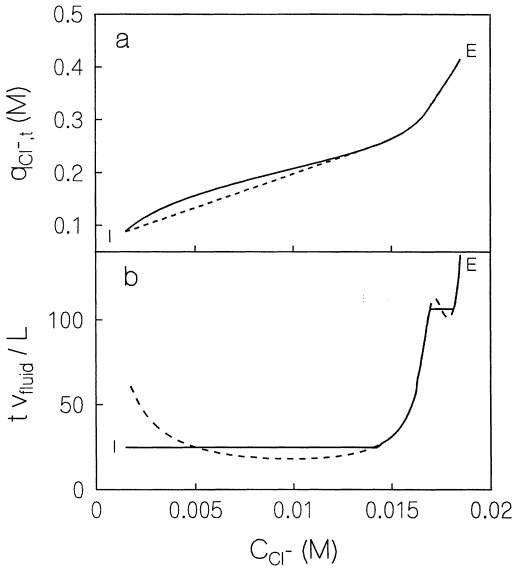

Fig. 10. Illustration of Golden's rule applied to an adsorption isotherm containing three inflection points. The conditions correspond to those used in Figs. 9 and 11 for the specific presaturation and elution conditions (points P and E) illustrated in those figures. The solid line in Fig. 10b shows the effluent concentration profile that results from using the actual isotherm in Fig. 10a, while the dotted line in Fig. 10b denotes the profile that results from using the effective isotherm in Fig. 10a. Physical properties used in the calculations are described in the caption to Fig. 11.

needed to determine the effluent pH profile. Fig. 11 shows experimental results, calculated results from LEQ theory, and results from a detailed numerical solution that accounts for mass transfer effects, all of which agree to within acceptable accuracy.

For the conditions corresponding to Figs. 10 and 11, the pH profile contains an initial steep portion corresponding to a self-sharpening (i.e., abrupt) section on the chloride adsorption isotherm, as illustrated specifically in Fig. 10a. Adjoined to the steep portion on the effluent pH profile is another portion where the pH changes in a gradual manner, corresponding to a non-selfsharpening section on the chloride adsorption isotherm. Finally, the pH profile terminates in a portion containing two smaller abrupt and gradual sections. The type of pH profile shown in Fig. 11 can be expected to be especially useful for the case where it is desired to focus certain proteins into narrow bands on the steeper sections of the profile, while at the same time isolating one or more proteins on the intermediate section of the profile as somewhat broader bands that are highly resolved from each other. Similar to the cases illustrated by Figs. 1 and 4 and by Figs. 6 and 7, the theoretical calculations shown in Figs. 9 and 10 were performed using only the acid–base equilibrium constants of the buffering species and the adsorption equilibrium data for the chloride ion shown in Fig. 2.

4.3. Protein separations

Figs. 12 and 13 illustrate two experiments where proteins were separated using retained pH gradients of the type discussed above. Fig. 12 in particular illustrates the separation of hemoglobin and myoglobin on a relatively steep pH profile extending between pH 9 and 7, while the separation of the A and B forms of β-lactoglobulin on a relatively broad pH gradient extending from pH 5 to 4 is illustrated in

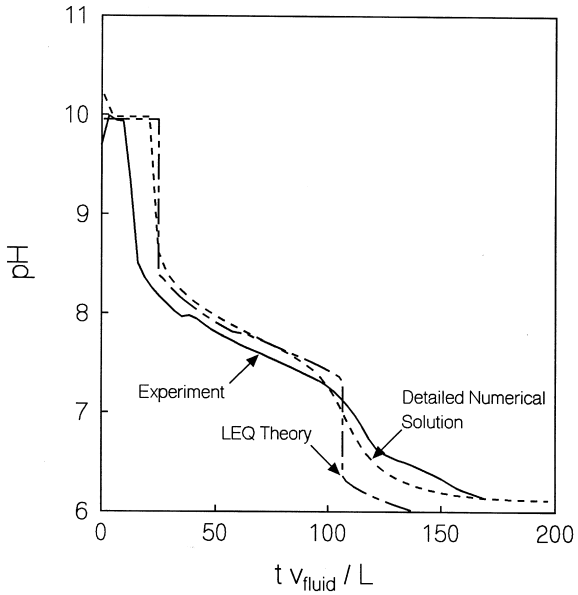

Fig. 11. Effluent pH profile obtained using a 12.8×1.0 cm column packed with PBE 94. The adsorbent was initially presaturated with 0.05 *M* DEA at a pH of 10.2 and eluted with a buffer containing 0.017 *M* DEA and 0.002 *M* Bis–Tris at a pH of 6.1 and a flow-rate of 1.0 ml/min. The pK_a values for Bis–Tris and DEA were taken as being 6.5 and 8.9, respectively. The adsorbent ion-exchange capacity and the adsorption equilibrium constants were the same as in Fig. 8. For the detailed numerical calculations, the intraparticle diffusion coefficient used for all of the buffering species and for the chloride ion was 10^{-6} cm^2/s, and the adsorption equilibrium constant for the neutral and positive forms of the buffering species were assumed to be unity.

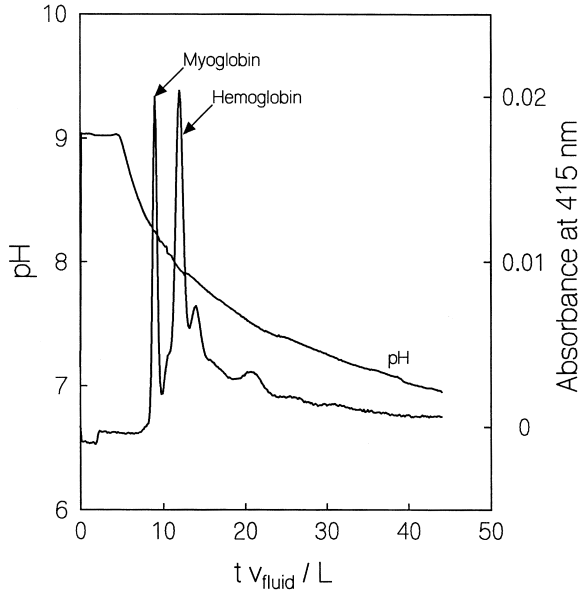

Fig. 12. Experimental separation of horse myoglobin and bovine hemoglobin accomplished by injecting a 0.5-ml feed sample containing 0.12 mg/ml myoglobin and 2.4 mg/ml hemoglobin on a 17×1.0 cm column packed with PBE 94. The column was initially presaturated with 0.02 *M* DEA at pH 9, and was eluted with a mixture of 0.02 *M* DEA, 0.002 *M* Tris[hydroxymethyl]aminomethane (Tris) and 0.004 *M* imidazole at pH 7 at a flow-rate of 0.75 ml/min.

Fig. 13. It can be seen in the figures that the proteins in these cases were well separated, especially considering the fact that the PBE column packing consists of particles having a relatively large diameter (45–160 μm), and despite the fact that the difference in pH where the proteins elute from the column is comparatively small, i.e., 0.3 and 0.2 pH units in Figs. 12 and 13, respectively. Further studies of the separation behavior of proteins in these types of systems, including the case when high performance column packings are employed, are currently underway as a follow-up study.

5. Conclusions

A buffer system was developed and investigated that permits gradual, quasi-linear pH gradients that are retained by an anion-exchange column packing to be produced by making a stepwise change from the presaturation to the elution buffer, and by using a small number of well-defined, non-adsorbed buffering species in these buffers. The pH profiles were shown to be suitable for the chromatofocusing separation of protein mixtures. A convenient local equilibrium theory was developed that can be used to optimize the shape of the pH gradient for a given desired separation.

6. Symbols

C_j	liquid phase concentration of species *j*, mol/l
$q_{k,t}$	adsorbed phase concentration, mol/l particle
$q^*_{k,t}$	equilibrium adsorbed phase concentration, mol/l particle

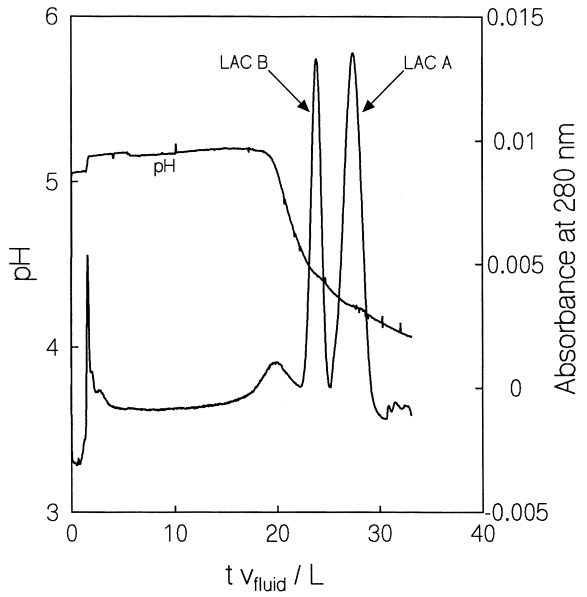

Fig. 13. Experimental separation of the A and B forms of β-lactoglobulin accomplished by injecting a 0.5-ml feed sample containing 1.0 mg/ml of an approximately equal mixture of the proteins on a 17×1.0 cm column packed with PBE 94. The column was initially presaturated with 0.005 *M* piperazine at pH 5 and was eluted with a mixture of 0.005 *M* piperazine and 0.003 *M* *n*-methylpiperazine at a flow-rate of 0.75 ml/min.

K_j	acid–base equilibrium constant of species *j*, mol/l
$K_{j,t}$	adsorption equilibrium constant based on total volume particle
z_j	charge of species *j*
q_{R_m}	concentration of adsorbing functional group *m*, mol/l particle
$q_{R^+,t}$	total charge on the adsorbent, mol/l particle
v_{fluid}, v_c	interstitial and concentration velocity, respectively, cm/s
t	time, s
z	axial distance, cm
L	column length, cm

Greek symbols

α	column void volume

Acknowledgements

Support from grant CTS 9414714 from the National Science Foundation is gratefully acknowledged.

References

[1] L.A.A.E. Sluyterman, O. Elgersma, J. Chromatogr. 150 (1978) 17.
[2] L.A.A.E. Sluyterman, J. Wijdenes, J. Chromatogr. 150 (1978) 31.
[3] L.A.A.E. Sluyterman, C. Koojstra, J. Chromatogr. 470 (1989) 317.
[4] D.D. Frey, A. Barnes, J. Strong, AIChE J. 41 (1995) 1171.
[5] D.D. Frey, Biotechnol. Prog. 12 (1996) 65.
[6] J. Strong, D.D. Frey, J. Chromatogr. A 769 (1997) 129.
[7] J.H. Scott, K.L. Kelner, H.P. Pollard, Anal. Biochem. 149 (1985) 163.
[8] M.T.W. Hearn, D.J. Lyttle, J. Chromatogr. 218 (1981) 483.
[9] T.W. Hutchens, C.M. Li, P.K. Besch, J. Chromatogr. 359 (1986) 157.
[10] T.W. Hutchens, C.M. Li, P.K. Besch, J. Chromatogr. 359 (1986) 169.
[11] K. Slais, J. Microcol. Sep. 3 (1991) 191.
[12] D. J. Kirsch, Mallinckrodt Baker Inc., personal communication, 1997.
[13] S.P. Mondarsh, E.A. Russoman, S.K. Roy, J. Chromatogr. 631 (1993) 277.
[14] P.C. Wankat, Rate Controlled Separations, Elsevier Applied Science, New York, 1990.
[15] D.D. Frey, Chem. Eng. Sci. 45 (1990) 131.
[16] F. Golden, Ph.D Thesis, University of California, Berkeley, 1973.
[17] D.D. Frey, Chem. Eng. Sci. 52 (1997) 1227.